Small Heteroborane Cluster Systems. 6. Mössbauer Effect Study of Iron Substituted Small Metallaborane Clusters

Bruce H. Goodreau,[†,‡] Lianna R. Orlando,[†,§] Gary J. Long,*[,⊥] and James T. Spencer*[,†]

Department of Chemistry and the W. M. Keck Center for Molecular Electronics, Center for Science and Technology, Syracuse University, Syracuse, New York 13244-4100, and Department of Chemistry, University of Missouri−Rolla, Rolla, Missouri 65401-0249

Received May 16, 1996[⊗]

The Mössbauer effect spectra for a series of small [Fe(η^5-C_5H_5)$(CO)_x$] substituted metallaborane complexes are reported, where $x = 1$ or 2. The pentaborane cage in compounds [Fe(η^5-C_5H_5)$(CO)_2B_5H_7P(C_6H_5)_2$] (**1**), [Fe(η^5-C_5H_5)$(CO)_2B_5H_8$] (**2**), and [(Fe(η^5-C_5H_5)$(CO)_2)_2B_5H_7$] (**3**) was found to act as a significantly better donor ligand than the ligands in a comparison group of previously reported [Fe(η^5-C_5H_5)(CO)LX] complexes, where L = CO or PPh_3 and X = halide, pseudohalide, or alkyl ligands. These metallaborane complexes were found to most resemble their silyl analogues in Mössbauer spectral parameters and the electronic distribution around the iron centers. In addition, the Mössbauer data showed that the [μ-2,3-$(P(C_6H_5)_2B_5H_7]^-$ ligand was a superior donor to the corresponding unsubstituted $[B_5H_8]^-$ ligand. The Mössbauer spectral results for the metallaborane complexes studied were found to be in general agreement with the anticipated donor and accepting bonding considerations for the cage ligands based upon their infrared and ^{11}B NMR spectra and X-ray structural features. The Mössbauer data for the [Fe(η^5-C_5H_5)$(CO)B_4H_6(P(C_6H_5)_2)$] (**4**) and [Fe(η^5-C_5H_5)$(CO)B_3H_7(P(C_6H_5)_2)$] (**5**) complexes, in comparison with compound **1**, showed that as the borane cage becomes progressively smaller, it becomes a poorer donor ligand. A qualitative relationship was found between the observed Mössbauer isomer shift data and the number of boron cage vertices for the structurally related [Fe(η^5-C_5H_5)$(CO)_xB_yH_zP(C_6H_5)_2$] complexes, where $x = 1$ or 2, $y = 3-5$, and $z = 6$ or 7. The X-ray crystallographic data for compounds **1**, **2**, **5**, and [Fe(η^5-C_5H_5)-$(CO)B_5H_8$] (**6**) were also found to agree with the trends observed in the Mössbauer spectra which showed that the s-electron density on the iron nucleus increases in the order **5** < **6** < **2** < **1**. The X-ray crystal structure of complex **2** is also reported. Crystallographic data for **2**: space group $P2_1/c$ (No. 14, monoclinic), $a = 6.084(3)$ Å, $b = 15.045(8)$ Å, $c = 13.449(7)$ Å, $\beta = 99.69(5)°$, $V = 1213(1)$ Å^3, $Z = 4$ molecules/cell.

Introduction

The structure and bonding of metallaborane complexes has been examined by a wide variety of both experimental and theoretical tools. Through this body of work, a great deal is now understood concerning how metal centers may interact with borane cages and how both electronic and orbital considerations influence the geometries and properties displayed by these complexes. Among the tools which have been most effectually employed in describing the electronic and structural properties of iron organometallic and metallaborane complexes, especially in combination with other spectroscopic techniques, is Mössbauer spectroscopy.

Mössbauer spectroscopy is a particularly useful technique for probing the local symmetry and electronic environment of metal centers in iron compounds. The Mössbauer effect involves nuclear transitions which arise from the absorption of γ-radiation by a sample.[1] These transitions are governed by the interactions of the nucleus with the surrounding electrons and electric field gradients. Because only s-electrons have a finite probability of existing at the nucleus, it is only these electrons that are responsible for the observed isomer shifts in the nuclear transitions. The s-electron density at the iron nucleus is, however, affected by the p and d orbital electron densities which shield the s-electrons from the full nuclear charge. In addition to the data regarding the s-electron distribution at the iron center, information about the local symmetry of the iron environment may be gained through the observed quadrupolar interactions. Thus, the Mössbauer effect isomer shifts, δ, and quadrupole splittings, ΔE_Q, have been particularly important in quantifying the interactions between an iron center and its ligand environment.

Numerous organoiron complexes, such as [Fe(η^5-C_5H_5)(CO)-LX], where L = CO and PPh_3 and X = halides, pseudohalides, alkyls, silyls, and boranes, and [Fe$(CO)_4L_x$] species, have been investigated using Mössbauer spectroscopy.[2−4] We have recently reported on the structures and photochemistry of a series of small metallaborane complexes of the type [Fe(η^5-C_5H_5)-$(CO)_x$L] (where $x = 1$ or 2 and L is a borane cage with between three and five boron vertices).[5−7] Issues of particular interest in these metallaborane complexes have related to how the metal−cage bonding is affected by changes in coordination mode of the cage to the iron center (terminal, bridged, inserted,

[†] Syracuse University.
[‡] Current address: Henkel Corp., Parker Amchem, 32100 Stevenson Highway, Madison Heights, MI 48071.
[§] National Science Foundation Research Experiences for Undergraduates Participant 1990−1991.
[⊥] University of Missouri, Rolla.
[⊗] Abstract published in *Advance ACS Abstracts,* October 1, 1996.

(1) Drago, R. S. *Physical Methods in Chemistry;* Saunder: Philadelphia, PA, 1977; pp 530−549.
(2) Pannell, K. H.; Wu, C. C.; Long, G. J. *J. Organomet. Chem.* **1980**, *186*, 85, and references cited therein.
(3) Long, G. J.; Alway, D. G, Barnett, K. W. *Inorg. Chem.* **1978**, *17*, 486.
(4) Coffy, T. J.; Medford, G.; Long, G. J.; Huffman, H. C.; Shore, S. G. *Organometallics* **1989**, *10*, 2404.
(5) Goodreau, B. H., Spencer, J. T. *Inorg. Chem*. **1991**, *30*, 2066.
(6) Goodreau, B. H.; Orlando, L. R.; Spencer, J. T. *J. Am. Chem. Soc.* **1992**, *114*, 3827.
(7) (a) Goodreau, B. H.; Orlando, L. R.; Spencer, J. T. *Inorg. Chem*. **1992**, *31*, 1731. (b) Goodreau, B. H.; Orlando, L. R.; Spencer, J. T. *J. Am. Chem. Soc.* **1995**, *117*, 11754.

S0020-1669(96)00547-2 CCC: $12.00

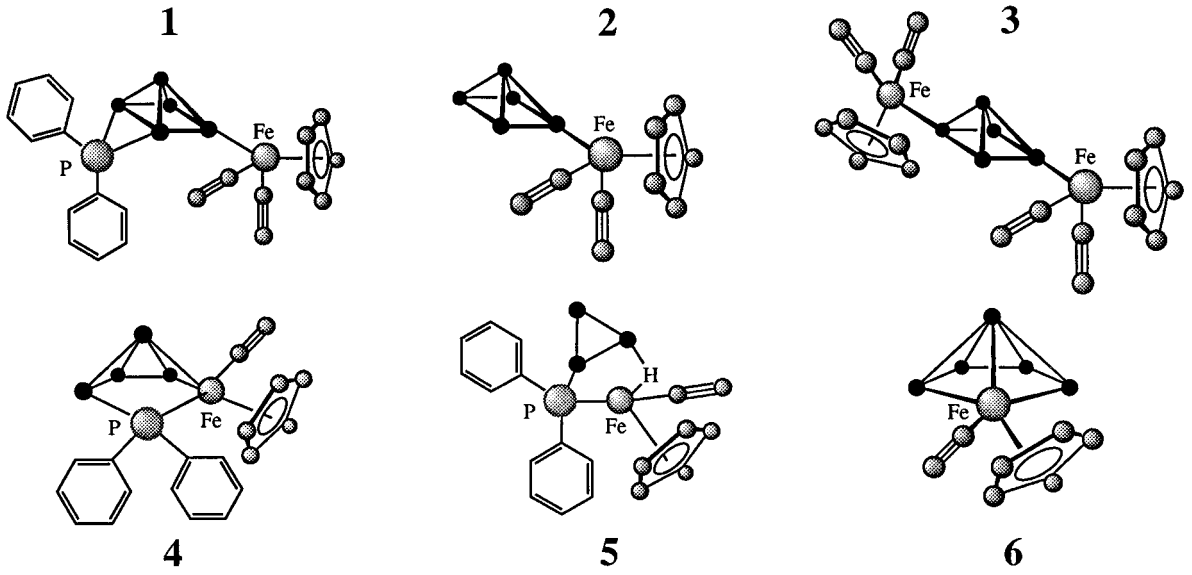

Figure 1. Structures of the iron substituted metallapentaborane clusters investigated: [Fe(η^5-C_5H_5)$(CO)_2B_5H_7P(C_6H_5)_2$] (**1**), [Fe(η^5-C_5H_5)$(CO)_2B_5H_8$] (**2**), [(Fe(η^5-C_5H_5)$(CO)_2)_2B_5H_7$] (**3**), [Fe(η^5-C_5H_5)$(CO)B_4H_6(P(C_6H_5)_2)$] (**4**), [Fe(η^5-C_5H_5)$(CO)B_3H_7(P(C_6H_5)_2)$] (**5**), and [Fe(η^5-C_5H_5)$(CO)B_5H_8$] (**6**). The boron atoms are indicated by the solid circles, and hydrogen atoms have been omitted for clarity.

etc.), how the cage size modifies these interactions, and what role exopolyhedral cage substitution plays in the nature of this iron−cage interaction. Direct information on some of these questions can be gained from Mössbauer spectral investigations of these metallaborane complexes.

In the work reported here, a series of iron substituted small metallaborane complexes with related structural features were first prepared. These [Fe(η^5-C_5H_5)$(CO)_x$] substituted metallaborane compounds, shown in Figure 1, include those which display a variety of bonding environments around the iron nucleus. In order to more fully understand the nature of the iron−cage bonding interaction, we found it useful to probe the electronic nature of the iron nucleus itself through observation of the Mössbauer spectra of these complexes (**1**−**6**). In the Mössbauer spectrum of an iron-57 compound, it is well-known that a decreasing isomer shift represents an increasing s-electron density at that iron nucleus.[8] The latter typically increases when a ligand donates electrons into an empty iron orbital through a σ-bond and/or a filled iron d orbital donates electron density into an empty ligand orbital through a π-bonding interaction. Although it is not possible to resolve the components of each of these bonding modes directly in the observed isomer shift, one can make qualitative observations relating the isomer shift to the chemical environment of the iron. Further insight into these metal−cage interactions may be gained from the ligands themselves which display NMR chemical shifts and infrared absorptions that are diagnostic of their local bonding environments relative to the iron nucleus. Relating the observed Mössbauer spectral parameters with the other spectroscopic data for the cage ligands can, therefore, provide a clearer overall picture of the bonding interactions between the ligand (borane cage) and the iron center. Thus, it was particularly interesting in the metallaborane complexes described here to explore the potential relationships between the Mössbauer spectral parameters and the ^{11}B NMR and infrared spectral data.

Experimental Section

Physical Measurements. Boron (^{11}B) NMR spectra were recorded on a Cryomagnetics spectrometer operating at 80.26 MHz. Spectra were recorded in 5 mm (o.d.) tubes in both the ^{1}H coupled and decoupled modes and were externally referenced to BBr_3 at +40.0 ppm (positive chemical shifts indicate downfield resonances). Carbon (^{13}C) NMR spectra were obtained on a General Electric QE-300 spectrometer operating at 75.48 MHz. The spectrometer was operated in the FT mode while locked on the deuterium resonance of either the $CDCl_3$ or tetrahydrofuran-d_8 (THF-d_8) solvent in 5 mm (o.d.) sample tubes. The reference was set relative to tetramethylsilane from the known chemical shifts of the solvent carbon atoms. Phosphorus (^{31}P) NMR spectra were obtained in 5 mm (o.d.) tubes on a Cryomagnetics spectrometer operating at 101.27 MHz. Chemical shifts were referenced to an external standard of 85% phosphoric acid sealed in a 1 mm capillary tube. Both proton broad-band decoupled and coupled spectra were routinely observed for each sample with a decoupling power of approximately 5 W. Proton (^{1}H) NMR spectra were obtained on a General Electric QE-300 spectrometer operating at 300.15 MHz. Spectra were recorded on samples dissolved in $CDCl_3$ or THF-d_8 in 5 mm (o.d.) tubes with chemical shifts referenced to internal tetramethylsilane with a positive shift indicating a resonance at a lower applied field than that of the standard. FT-IR spectra in the range of 400−4000 cm^{-1} were measured on a Mattson Galaxy 2020 spectrometer and were referenced to the 1601.8 cm^{-1} band of polystyrene. All compounds were recorded as Nujol mulls sandwiched between NaCl plates.

The Mössbauer effect spectra were measured on a constant acceleration spectrometer which utilized a room temperature rhodium matrix cobalt-57 source and was calibrated at room temperature with a natural α-iron foil. The spectra were fit with symmetric quadrupole doublets by using standard least squares fitting procedures.

Materials. All solvents used were of reagent grade or better. THF and pentane were distilled from sodium metal/benzophenone under a dry nitrogen atmosphere prior to use. Methylene chloride and hexane were used as received. All organic solvents, after appropriate drying, were degassed by repeated freeze−evacuate−thaw cycles and finally stored *in vacuo* prior to use.[9] Deuterated solvents were vacuum distilled onto 4 Å molecular sieves prior to use. *nido*-Pentaborane(9) was taken directly from our laboratory stock. The compounds [Fe(η^5-C_5H_5)-$(CO)_2B_5H_7P(C_6H_5)_2$] (**1**),[5] [(Fe(η^5-C_5H_5)$(CO)_2)_2B_5H_7$] (**3**),[10] [Fe(η^5-C_5H_5)$(CO)B_4H_6(P(C_6H_5)_2)$] (**4**),[6] [Fe(η^5-C_5H_5)$(CO)B_3H_7(P(C_6H_5)_2)$] (**5**),[6] and [Fe(η^5-C_5H_5)$(CO)B_5H_8$] (**6**)[7] were prepared and purified according to previously reported literature methods. The spectroscopic data for these compounds matched those previously reported. The following commercially available anhydrous chemicals were either used as received or purified by the method indicated and, where possible, were

(8) Bancroft, G. M. *Mössbauer Spectroscopy;* Wiley: New York, 1973.

(9) Shriver, D. F.; Drezdzon, M. S. *The Manipulation of Air-Sensitive Compounds*, 2nd ed.; Wiley-Interscience: New York, 1986.

stored over 4 Å molecular sieves prior to use: $[Fe(\eta^5\text{-}C_5H_5)(CO)_2]_2$ (Strem), iodine (Aldrich), $ClP(C_6H_5)_2$ (Aldrich), $ClP(O)(C_6H_5)_2$ (Aldrich), and sodium hydride (Aldrich) (the 80% suspension in mineral oil was washed several times with dry pentane and the washes decanted off to remove the mineral oil). Analytical thin-layer chromatography was conducted on 2.5 × 7.5 cm silica gel strips (1B-F, Baker), and conventional column chromatography was conducted using 4.0 × 20 cm columns packed with 230−400 mesh (ASTM) silica gel (EM Science).

$[2\text{-}(Fe(\eta^5\text{-}C_5H_5)(CO)_2)B_5H_8]$ (2). In the preparation of complex **2**, a modification of the procedure previously reported independently by Greenwood and Gaines was employed.[10] In our work, a B_5H_9/THF stock solution was employed[11] rather than using the high vacuum line techniques previously described. In a typical reaction, 17.8 mL of a 0.56 M B_5H_9/THF solution was deprotonated with 0.3 g (10 mmol) of NaH in 40 mL of THF under a dry nitrogen atmosphere at −50 °C. This $Na[B_5H_8]$/THF solution was added to a second solution containing 3.03 g (10 mmol) of $[Fe(\eta^5\text{-}C_5H_5)(CO)_2I]$ in 60 mL of THF at −78 °C under a dry N_2 atmosphere. The mixture was stirred for 2 h and then warmed slowly to room temperature. The solvent was removed by vacuum distillation, and the residue was extracted with 2 × 60 mL of pentane to give pure **2** (2.21 g, 92% yield). The spectroscopic data for **2** matched those previously reported.[10,7b]

X-ray Crystallography of 2. A red 0.4 × 0.2 × 0.2 mm crystal of $[2\text{-}(Fe(\eta^5\text{-}C_5H_5)(CO)_2)B_5H_8]$ (**2**) was grown by allowing a pure sample of the compound to stand in a sealed vial under vacuum at room temperature for 2 weeks. The low melting point of **2** apparently allowed the sample to melt and resolidify as well-formed crystals. The crystal was mounted in a 0.3 mm Lindemann capillary tube and sealed under an inert, dry nitrogen atmosphere. All measurements were made on a Rigaku AFC5S diffractometer at −10 °C using graphite monochromated Mo Kα radiation (λ = 0.710 73 Å). Cell constants and an orientation matrix for the data collection were obtained from a least squares refinement using 25 centered reflections in the range of $10.7° < 2\theta < 22.0°$. On the basis of the systematic absences of $h0l$, $l \neq 2n$, and $0k0$, $k \neq 2n$, and the successful structural solution, the space group was uniquely determined to be $P2_1/c$. Data were collected at room temperature using an $\omega-2\theta$ scan technique to a maximum 2θ value of 60.0°. Three reference reflections were monitored every 100 reflections during the data collection and no significant intensity variation occurred. The data reduction of 3993 measured reflections resulted in 3684 unique reflections ($R_{int.}$ = 0.033). There were 2114 independent reflections with $I > 3\sigma(I)$ in the range of $2\theta < 60°$ which were used for the structure refinement (reflection/parameter = 12.58). The position of the iron atom was determined from a Patterson synthesis, and the remaining non-hydrogen atoms were located by application of direct methods to generate a trial structure.[12,13] The non-hydrogen atoms were refined anisotropically. The boron cage hydrogen atoms were then located by difference maps and were refined isotropically. All other hydrogen atoms were calculated and refined isotropically. The final cycle of a full-matrix least squares refinement converged with $R = [(\sum(|F_o| - |F_c|)^2/\sum(Fo)^2]^{1/2} = 0.041$ and $R_w = [(\sum w(|F_o| - |F_c|)^2/\sum w(F_o)^2]^{1/2} = 0.045$. The final structure was plotted using the Texsan[14] graphics programs, including PLUTO[15] and ORTEP.[16] The crystallographic data, bond lengths and bond angles for **2** are given in Tables 1−3. The crystallographic data, atomic positional parameters, anisotropic thermal parameters, bond distances and angles involving both non-hydrogen and hydrogen atoms, and intermolecular distances for **2** are available as Supporting Information.

Table 1. Crystallographic Data for $[Fe(\eta^5\text{-}C_5H_5)(CO)_2B_5H_8]$ (**2**)

chem formula	$C_7H_{13}B_5FeO_2$	diffractometer	Rigaku AFC5S
fw	239.08	ρ_{calcd} (g cm^{-3})	1.309
cryst syst	monoclinic	μ (cm^{-1})	12.11
space group	$P2_1/c$ (No. 14)	transm coeff	
temp (K)	263	Ψ	0.9556−1.0000
cell dimensions		Ψav	0.9793
(at 263 K)		R	0.041
a (Å)	6.084(3)	R_w	0.045
b (Å)	15.045(8)	total no. of reflcns	3993
c (Å)	13.449(7)	no. of reflcn with $I > 3\sigma(I)$	2114
α (deg)	90.00		
β (deg)	99.69(5)	no. of variables	168
γ (deg)	90.00	$2\theta_{max}$ (deg)	60.0
V (Å^3)	1213(1)	goodness of fit	1.66
Z molecules/cell	4	max shift/error in final cycle	0.10
λ(Mo Kα) (Å)	0.710 73		

Table 2. Intramolecular Bond Distances[a] for $[Fe(\eta^5\text{-}C_5H_5)(CO)_2B_5H_8]$ (**2**)

Fe(1)−B(2)	2.035(3)	B(2)−B(3)	1.821(5)
Fe(1)−C(1)	1.734(3)	B(2)−B(5)	1.825(5)
Fe(1)−C(2)	1.738(4)	B(1)−B(3)	1.655(6)
Fe(1)−C(6)	2.062(4)	B(1)−B(5)	1.656(6)
Fe(1)−C(3)	2.062(4)	B(1)−B(2)	1.690(5)
Fe(1)−C(4)	2.084(4)	B(1)−B(4)	1.675(6)
Fe(1)−C(7)	2.071(4)	B(4)−B(3)	1.790(7)
Fe(1)−C(5)	2.082(4)	B(4)−B(5)	1.777(7)
C(6)−C(7)	1.403(8)	B(3)−H(23)	1.22(4)
C(6)−C(5)	1.383(7)	B(3)−H(34)	1.34(4)
C(3)−C(4)	1.314(8)	B(1)−H(1)	1.05(3)
C(3)−C(7)	1.365(8)	B(2)−H(25)	1.35(4)
C(4)−C(5)	1.289(7)	B(2)−H(23)	1.35(3)
C(5)−H(50)	0.952	B(5)−H(25)	1.24(4)
C(7)−H(49)	0.950	B(5)−H(45)	1.20(4)
C(6)−H(46)	0.950	B(5)−H(5)	1.07(4)
C(4)−H(48)	0.951	B(3)−H(3)	1.10(4)
C(3)−H(47)	0.951	B(4)−H(4)	1.01(4)
C(1)−O(1)	1.151(4)	B(4)−H(34)	1.18(4)
C(2)−O(2)	1.148(4)		

[a] Distances are in angstroms. The estimated standard deviations in the least significant figure are given in parentheses.

Table 3. Selected Intramolecular Bond Angles[a] for $[Fe(\eta^5\text{-}C_5H_5)(CO)_2B_5H_8]$ (**2**)

B(2)−Fe(1)−C(1)	84.1(1)	B(2)−Fe(1)−C(2)	83.1(1)
Fe(1)−B(2)−B(2)	136.2(2)	Fe(1)−B(2)−B(3)	136.2(2)
Fe(1)−B(2)−B(5)	136.2(2)	B(1)−B(2)−B(3)	56.1(2)
B(1)−B(2)−B(5)	56.1(2)	B(3)−B(2)−B(5)	87.3(3)
C(1)−Fe(1)−C(2)	94.3(2)	Fe(1)−C(1)−O(1)	179.4(4)
Fe(1)−C(2)−O(2)	178.8(4)	B(2)−B(1)−B(4)	100.3(3)
B(2)−B(1)−B(3)	65.9(2)	B(2)−B(1)−B(5)	66.1(2)
B(4)−B(1)−B(3)	65.0(3)	B(4)−B(1)−B(5)	64.5(3)
B(3)−B(1)−B(5)	98.9(3)	B(1)−B(4)−B(3)	56.9(2)
B(1)−B(4)−B(5)	57.3(2)	B(3)−B(4)−B(5)	89.7(3)
B(2)−B(3)−B(1)	57.9(2)	B(2)−B(3)−B(4)	91.4(3)
B(2)−B(5)−B(1)	57.8(2)	B(2)−B(5)−B(4)	91.6(3)
B(1)−B(5)−B(4)	58.3(3)	B(1)−B(3)−B(4)	58.0(3)

[a] Angles are in degrees. Estimated standard deviations in the least significant figure are given in parentheses.

Results and Discussion

All of the small metallaborane compounds studied in this work were found to display well-resolved Mössbauer spectra consisting of quadrupole doublets with splittings ranging from 1.58 to 1.96 mm/s. Spectra which are typical of the complexes investigated here are illustrated in Figure 2 by those obtained for compounds $[Fe(\eta^5\text{-}C_5H_5)(CO)_2B_5H_7P(C_6H_5)_2]$ (**1**) and $[(Fe(\eta^5\text{-}C_5H_5)(CO)_2)_2B_5H_7]$ (**3**) at both 295 and 78 K. The room

(10) (a) Fischer, M. B.; Gaines, D. F.; Ulman, J. A. *J. Organomet. Chem.* **1982**, *231*, 55. (b) Greenwood, N. N.; Kennedy, J. D.; Savory, C. G.; Staves, J.; Trigwell, K. R. *J. Chem. Soc., Dalton Trans.* **1978**, 237.
(11) Cendrowski-Guillaume, S. M.; Spencer, J. T. *Organometallics* **1992**, 11, 969.
(12) Calbrese, J. C. PHASE. Patterson Heavy Atom Solution Extractor. Ph.D. Dissertation, University of Wisconsin, Madison, WI, 1972.
(13) Beurskens, P. T. DIRDIF. Direct Methods for Difference Structures. Technical Report. 1984/1; Crystallography Laboratory: Toernooiveld, Nijmegen, Netherlands.
(14) TEXSAN. Texray Structure Analysis Package; Molecular Structure Corp.: 1985.
(15) Motherwell, S.; Clegg, W. Pluto. Program for plotting molecular and crystal structures, University of Cambridge: Cambridge, England, 1978.
(16) Johnson, C. K. ORTEPII; Report ORNL-5138; Oak Ridge National Laboratory: Oak Ridge, TN, 1976.

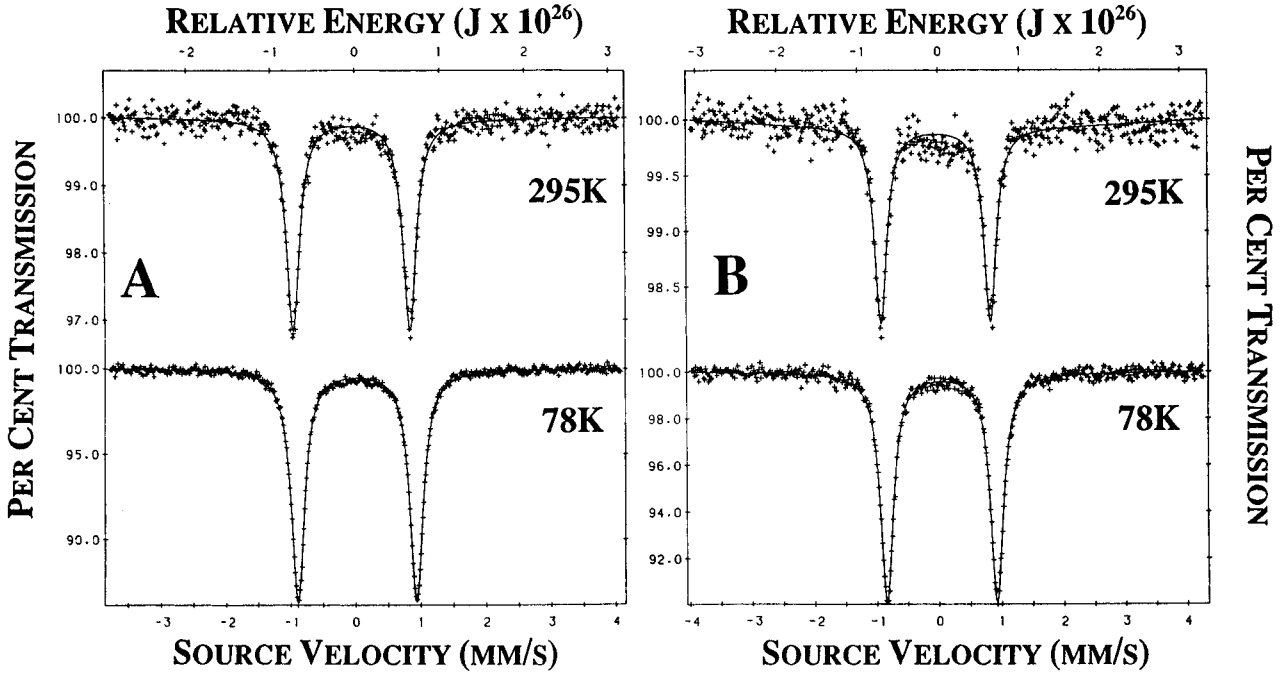

Figure 2. Mössbauer spectra of complexes (A) [Fe(η^5-C_5H_5)$(CO)_2B_5H_7P(C_6H_5)_2$] (**1**) and (B) [(Fe(η^5-C_5H_5)$(CO)_2)_2B_5H_7$] (**3**) measured at both 295 and at 78 K.

Table 4. Mössbauer Effect Spectral Parameters for the Iron Substituted Metallaborane Clusters[a]

compound	T (K)	δ[a] (mm/s)	ΔE_Q (mm/s)	Γ (mm/s)	area (%)	abs area (%ϵ) (mm/s)	M_{eff} (g/mol)	Θ_M (K)
[Fe(η^5-C_5H_5)$(CO)_2B_5H_7P(C_6H_5)_2$] (**1**)	295	-0.056	1.80	0.25	100	2.39	113	100
	78	0.024	1.82	0.25	100	10.45		
[Fe(η^5-C_5H_5)$(CO)_2B_5H_8$] (**2**)	78[b]	0.039	1.84	0.27	100	13.15	–	–
[(Fe(η^5-C_5H_5)$(CO)_2)_2B_5H_7$] (**3**)	295	-0.046	1.76	0.24	100	1.28	106	93
	78	0.039	1.77	0.25	100	7.56		
[Fe(η^5-C_5H_5)$(CO)B_4H_6(P(C_6H_5)_2)$] (**4**)	78[b]	0.124	1.75	0.29	100	6.93	–	–
[Fe(η^5-C_5H_5)$(CO)B_3H_7(P(C_6H_5)_2)$ (**5**)	295	0.162	1.94	0.25	100	0.64	109	101
	78	0.245	1.96	0.26	100	2.42		
[Fe(η^5-C_5H_5)$(CO)B_5H_8$] (**6**)	295	0.005	1.66	0.32	100	0.23	92	74
	78	0.077	1.58	0.32	74	5.11		
		0.151	1.91	0.32	17	1.15		
		0.234	2.07	0.32	9	0.65		

[a] Relative to natural α-iron foil. [b] No 295 K spectrum was observed.

temperature spectra for complexes **2** and **4** were not observed because they melt either near or at room temperature. With the exception of **6**, all of the complexes gave clean spectra at 78 K. At this temperature, complex **6** gave an asymmetric broadened quadrupole splitting which could best be fit with three symmetric quadrupole doublets with decreasing area as the splitting increased. These different components may arise from different isomers of **6** which may exist in the solid state, isomers in which the bridging hydrogens in the FeB_5H_8 moiety may bridge between a boron and iron rather than between two boron sites to give an iron with no bonded hydrogen (74% of the compound), one bonded hydrogen (17% of the compound), and two bonded hydrogens (9% of the compound). Although this deconvolution of the spectrum may not be unique, it does explain well the observed spectral line shape at 78 K in terms of realistic structural isomers.

The experimental Mössbauer spectral parameters for compounds **1**−**6** are given in Table 4. For these complexes, the 78 K isomer shift was found to decrease through the series in the order **5** > **4** > **6** > **3** = **2** > **1**. Also, the quadrupole splittings were observed to decrease in the order **5** > **2** > **1** > **3** > **4** > **6**. The magnitudes and range of these spectral parameters were in the general range of those previously reported for a series of [Fe(η^5-C_5H_5)$(CO)_2$R] complexes (where R = alkyl or silyl groups).[2] When it has been possible to observe both a room temperature and a 78 K Mössbauer spectrum, we have used the temperature dependence of the isomer shift and the logarithm of the spectral absorption area to calculate the effective recoil masses of the iron, m_{eff}, and the Mössbauer temperature, Θ_M, for the complex.[17] The resulting values, given in Table 4, are typical of organoiron complexes and indicate extensive covalency in the iron−ligand bonds, a covalency which is the smallest in complex **6**.[18]

There have been extensive Mössbauer studies of [Fe(η^5-C_5H_5)(CO)LX] compounds, where L = CO and PPh_3 and X = halides, pseudohalides, alkyls, and silyls.[2−4] The Mössbauer spectral parameters for several selected compounds of this type are given in Table 5. It is well-known that an increase in the s-electron density at an iron nucleus will result in a decrease in the Mössbauer isomer shift.[3] This s-electron density increase is generally regarded to result from either a σ-donation of electron density from the ligand to the metal or a π-back-bond donation of electron density from a metal filled d orbital into a suitable acceptor orbital on the ligand. Thus, poor σ-donor and

(17) Herber, R. H. In *Chemical Mössbauer Spectroscopy*; Herber, R. H., Ed.; Plenum: New York, 1984; p 199.
(18) Ernst, R. D.; Wilson, D. R.; Herber, R. H. *J. Am. Chem. Soc.* **1984**, *106*, 1646.

Table 5. Mössbauer and Infrared Spectral Data for Selected Known Organometallic Iron Compounds

compound	δ^a (78 K)	$\Delta E_Q{}^b$	Γ^c	ν(CO)^d	ref
$Fe(\eta^5\text{-}C_5H_5)(CO)_2(\eta^2\text{-}B_2H_5)$	0.072	1.68	0.27	2045, 1990	4
$[Fe(\eta^5\text{-}C_5H_5)(CO)_2(\eta^2\text{-}B_2H_5)]^-$	−0.14	1.33	0.31	2030, 1943, 1927	4
$[Fe(CO)_4(B_6H_{10})]^e$	−0.4	1.71			19
$Fe(\eta^5\text{-}C_5H_5)(CO)_2SiPh_3$	0.039	1.80	0.24	2001, 1953	2
$Fe(\eta^5\text{-}C_5H_5)(CO)_2SiCH_3$	0.046	1.76	0.27	1996, 1944	2
$Fe(\eta^5\text{-}C_5H_5)(CO)_2CH_3$	0.076	1.76	0.26	2010, 1957	2
$Fe(\eta^5\text{-}C_5H_5)(CO)_2CH_2(C_6H_5)$	0.081	1.74	0.26	2009, 1960	2
$Fe(\eta^5\text{-}C_5H_5)(CO)_2Br$	0.227	1.87	0.35	2045, 1999	3
$Fe(\eta^5\text{-}C_5H_5)(CO)(Ph_3P)Br$	0.290	1.89	0.26	1960	3
$Fe(\eta^5\text{-}C_5H_5)(CO)_2I$	0.215	1.84	0.28	2038, 1998	3
$Fe(\eta^5\text{-}C_5H_5)(CO)(Ph_3P)I$	0.308	1.87	0.28	1955	3
$[Fe(\eta^5\text{-}C_5H_5)(CO)_3]PF_6$	0.046	1.88	0.26	2125, 2079	3
$[Fe(\eta^5\text{-}C_5H_5)(CO)_2(Ph_3P)]PF_6$	0.085	1.82	0.28	2055, 2010	3

[a] Mössbauer isomer shift (mm/s), not to be confused with the chemical shift in NMR which uses the same symbol. [b] Quadrupole splitting (mm/s). [c] Line width (mm/s). [d] Infrared carbonyl stretching frequency (cm^{-1}). [e] ^{11}B NMR chemical shift of the boron atom(s) adjacent to the iron nucleus (ppm).

Table 6. Observed Mössbauer, Infrared, and ^{11}B NMR Spectral Data for Iron Substituted Metallaborane Clusters

compound	site	δ(78K)^a (mm/s)	ΔE_Q (mm/s)	Γ (mm/s)	ν(CO)^d (cm^{-1})	^{11}B NMR^b	ref
$[Fe(\eta^5\text{-}C_5H_5)(CO)_2B_5H_7P(C_6H_5)_2]$ (**1**)		0.024	1.82(1)	0.25	1990, 1934	23.3	this work
$[Fe(\eta^5\text{-}C_5H_5)(CO)_2B_5H_8]$ (**2**)		0.039	1.84	0.27	2005, 1947	7.9	this work
$[(Fe(\eta^5\text{-}C_5H_5)(CO)_2)_2B_5H_7]$ (**3**)		0.039	1.77	0.25	1996, 1936	2.7	this work
$[Fe(\eta^5\text{-}C_5H_5)(CO)B_4H_6(P(C_6H_5)_2)]$ (**4**)		0.129	1.75	0.29	1948	30.2, −21.2	this work
$[Fe(\eta^5\text{-}C_5H_5)(CO)B_3H_7(P(C_6H_5)_2)]$ (**5**)		0.244	1.96	0.26	1962	9.1	this work
$[Fe(\eta^5\text{-}C_5H_5)(CO)B_5H_8]$ (**6**)		0.104[c]	1.68[c]	0.32	1940	+76.0	this work
$[Fe_2(CO)_6(B_2H_6)]$	Fe(HHFe)	−0.02	1.24	0.24	2090, 2046	−24.2	21
	Fe(HBFe)	0.05	1.08	0.48	2024,1993		
$[Fe_2(CO)_6(B_2H_5)][PPN]$	Fe(HHFe)	−0.01	1.27	0.28	2022, 1965	−17.4	21
	Fe(HBFe)	0.05	1.44	0.23	1935, 1928		
	Fe(BBFe)	0.10	0.22	0.42			
$[Fe_3(\mu\text{-}H)(CO)_9BH_3][PPN]$	Fe(1,3)	0.009	0.45	0.47	2045, 1954	6.2	22
	Fe(2)	−0.042	1.10	0.34			
$[[Fe_4H(CO)_{12}BH][PPN]$	Fe(1,3)	−0.03	0.65	0.44	2003, 1983	150	23
	Fe(2)	−0.06	1.86	0.24			
	Fe(4)	−0.03	1.06	0.38			
$[Fe(CO)_4(B_6H_{10})]^d$		−0.40[d]	1.71[d]		2078, 2018, 1986, 1981	−0.2 or −4.9	20
$[Fe(B_{10}H_{10}S)_2]Cs_2$		0.21	2.14	0.32			24
$[Fe(B_{10}H_{10}S)_2][N(CH_3)_4]$		0.23	2.25	0.29			24
$[Fe(C_2B_9H_{11})_2]Cs_2$		0.25	2.38	0.36			24
$[Fe(C_2B_9H_{11})_2][N(CH_3)_4]$		0.30	2.80[d]	0.27			25

[a] Mössbauer isomer shift (mm/s), not to be confused with the chemical shift in NMR which uses the same symbol. [b] ^{11}B NMR chemical shift of the boron atom(s) adjacent to the iron nucleus (ppm). [c] Area weighted average values. [d] The temperature of these spectra are not specified but are probably room temperature spectra.

poor π-acceptor ligands produce the highest isomer shifts, whereas good σ-donors and good π-acceptors typically produce the lowest isomer shifts values.[3] For the $[Fe(\eta^5\text{-}C_5H_5)(CO)\text{-}LX]$ complexes previously reported, the isomer shifts for the carbon monoxide substituted compounds were found to be typically lower than their phosphine counterparts.[2] This has been interpreted to indicate that there is a greater s-electron density at the iron nucleus in the $[Fe(\eta^5\text{-}C_5H_5)(CO)_2X]$ complexes than in the analogous $[Fe(\eta^5\text{-}C_5H_5)(CO)(PPh_3)X]$ compounds. This observation is consistent with the well-supported concept that CO is a significantly better π-acceptor ligand than the PPh_3 ligand.[19]

Our studies with the iron-substituted small metallaborane complexes **1**−**6** revealed the same general trends concerning the relative π-acceptor strengths of the carbonyl and phosphine ligands toward the iron as those cited above. Compounds **1**−**3**, in which the coordination sphere around the iron consists of two CO ligands and the cage, were found to have lower isomer shifts than complexes **4** and **5**, in which the coordination sphere around the iron consists of one carbonyl ligand, one phosphine ligand, and the cage. In addition, compounds **1**−**3** were found to have smaller isomer shifts than their corresponding halide, pseudohalide, or alkyl complexes. The isomer shifts for complexes **1**−**3** were most similar to those observed for the $[Fe(\eta^5\text{-}C_5H_5)(CO)(PPh_3)SiPh_3]$ and $[Fe(\eta^5\text{-}C_5H_5)(CO)_3][PF_6]$ complexes.[2]

In view of the low observed isomer shifts for the metallapentaborane complexes **1**−**3**, the pentaborane ligand must either be a better donor and/or a better acceptor than the analogous halide, pseudohalide, or alkyl ligands. If the pentaborane cage is a better donor ligand, then the observed carbonyl stretching frequency in the infrared spectrum should be lower in compounds **1**−**3** than in the corresponding halide, pseudohalide, or alkyl complexes because of the localization of a greater amount of electron density on the iron available for π-bonding to the carbonyl. In contrast, if the borane cage is a stronger acceptor in compounds **1**−**3**, then the carbonyl stretching frequency would be expected to be higher than the corresponding halide, pseudohalide, or alkyl complexes because less electron density is available for π-back-bonding from the iron into the π^* orbital of the carbonyl ligand. The observed infrared carbonyl stretching frequencies in compounds **1**−**3**, given in Tables 5 and 6, are clearly lower than those in the comparison group, suggesting that the pentaborane cage is primarily a better donor ligand relative to this group. While borane clusters are often incorrectly

(19) (a) Eaton, G. R.; Lipscomb, W. N. *NMR Studies of Boron Hydrides and Related Compounds*; Benjamin: New York, 1969. (b) Todd, L. J.; Siedle, A. R. *Prog. NMR Spectrosc.* **1979**, *13*, 87.

regarded as "electron deficient" species, because they apparently have fewer valence electrons than valence orbitals and require the use of multicenter bonding schemes, it is far more accurate to view them as relatively electron rich, delocalized systems capable of significant electron donation toward external metal centers, as is evidenced in the observed Mössbauer spectral isomer shifts in compounds **1**−**3** reported here.

Comparisons of the infrared and ^{11}B NMR spectroscopic data with the Mössbauer parameters for the σ-bound [Fe(η^5-C_5H_5)-$(CO)_2$(cage)] complexes **1**−**3**, given in Table 6, are consistent with the trends anticipated. Of the three complexes, (**1**) had the lowest isomer shift and the lowest carbonyl stretching frequency. This is consistent with the idea that the [μ-2,3-$(P(C_6H_5)_2)B_5H_7]^-$ ligand is a better donor than $[B_5H_8]^-$, as expected on the basis of the presumed electron donating properties of the bridging phosphine cage substitutent. The Mössbauer spectral parameters are also consistent with the observed ^{11}B NMR chemical shifts for these complexes. Compound **1,** which contains the best σ-donating borane ligand, had the smallest observed isomer shift and the largest downfield chemical shift in the ^{11}B NMR (δ = 23.3 ppm).

The isomer shifts for compounds **4** and **5** indicate that these complexes have significantly less s-electron density at the iron nucleus than do compounds **1**−**3**. The phosphino bridged compounds **1**, **4**, and **5** have very different isomer shifts ranging over an order of magnitude from 0.024 mm/s to 0.244 mm/s, a range which presumably must be the result of the different sized borane cage ligands present in the complexes. Although a comparison of only three compositionally analogous [Fe(η^5-C_5H_5)$(CO)_2$(cage)] complexes in which the cage decreases in size from five to three boron vertices is possible here, an interesting qualitative trend was observed for these species in the Mössbauer spectral data in which the isomer shifts decrease linearly as the cage becomes progressively smaller. While detailed considerations of this trend are not possible due to the widely differing cage−metal center interactions, such a general decrease in the isomer shifts would be anticipated because the cage should become a poorer electron donor as it becomes smaller. Further qualitative support for this analysis is obtained from infrared data which indicates that the $B_4H_6PPh_2^-$ ligand in **4** is a better donor than the $B_3H_7PPh_2^-$ ligand in **5** because the carbonyl absorption frequency in **4** is significantly lower than that of **5**.

It is useful to compare the observed Mössbauer spectral parameters for the metallaborane complexes with their X-ray crystallographically determined bond distances and angles. The crystal structures for compounds **1**, **5**, and **6** have been reported previously.[5,6,7b] Particularly useful in comparison with these complexes, however, is the crystallographic data for compound **2**, because it represents the direct analogue of compound **1** in which the μ-2,3-($P(C_6H_5)_2$) unit of **1** has been replaced by a bridging μ-B−H−B unit in compound **2**. The X-ray structure of compound **2** has not been reported previously.

Compound **2** was formed in high yield from the reaction of [Fe(η^5-C_5H_5)$(CO)_2$I] with Na[B_5H_5] in THF at low temperature.[10] The ^{11}B NMR spectrum of the complex, with four resonances in a 2:1:1:1 ratio, is indicative of a basal substitution of a [Fe(η^5-C_5H_5)$(CO)_2$] unit in a terminal position. The farthest downfield peak was observed as a singlet in both the ^{1}H coupled and decoupled modes (δ = 7.9 ppm). Also, the ^{11}B NMR chemical shift of this peak is >20 ppm downfield from the equivalent basal boron resonance in B_5H_9 (δ = −12.6 ppm).[20]

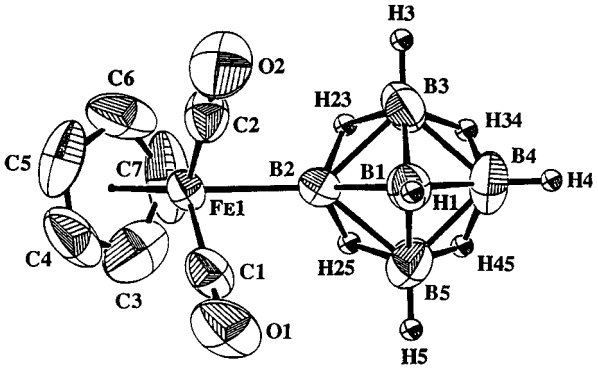

Figure 3. ORTEP drawing of [2-Fe(η^5-C_5H_5)$(CO)_2B_5H_8$] (**2**) showing the atomic numbering scheme. The thermal ellipsoids are drawn at the 50% probability level. The hydrogen atoms of the C_5H_5 ring have been omitted for clarity.

On the basis of these observations, the resonance at 7.9 ppm was assigned spectroscopically to the terminal iron-substituted basal boron atom (B(2)).[10] A single crystal X-ray structural analysis confirmed that **2** was indeed a 2-substituted terminally bound metallapentaborane. The atom numbering scheme and molecular structure for **2** is given in Figure 3. Crystallographic data, bond lengths, and bond angles are given in Tables 1−3. The [Fe(η^5-C_5H_5)$(CO)_2$] unit in **2** is σ-bound to a single basal boron atom of a square pyramid of boron atoms. The iron may be thought of as displaying a distorted tetrahedral geometry coordinated to two carbonyl ligands, the pentaborane cage, and the centroid of the cyclopentadienyl ring. The bond lengths and angles of the molecule are typical of other molecules which contain either the [Fe(η^5-C_5H_5)$(CO)_2$] or [B_5H_8] fragments. In contrast with the large distortion in the structure previously reported for **1**, there is relatively little distortion in the square pyramidal pentaborane cage in the crystal structure of **2**.[5] The B(1)−B(basal) bond distances in **2** are all approximately the same, ranging from 1.655 to 1.690 Å. The [Fe(η^5-C_5H_5)$(CO)_2$] fragment apparently causes relatively little distortion of the cage bonding relative to the parent *nido*-B_5H_9 cluster. There are, however, small inductive effects in operation because the B(1)−B(2) distance of 1.69 Å is the longest of the four B−B distances.

The X-ray structural results for compounds **1**, **2**, **5**, and **6** were found to agree with the general analysis that the s-electron density on the iron nucleus increases in the order **5** < **6** < **2** < **1**, as observed in the Mössbauer spectral results. The carbonyl C−O bond distances increase in exactly this same order, as is shown in Table 7. While there is a general increase in the CO bond distance with decreasing isomer shift, δ, the magnitude of the change of the CO bond distance is not as striking as the differences observed between isomer shifts for these compounds. The diminution of the changing electron distribution effect in the carbonyl bond distances probably results because changes in electron density at iron, as measured directly in the isomer shift, are distributed among the entire ligand sphere of the metal and not localized solely in the Fe−CO interaction. Thus, while the isomer shift directly measures the effect of changing the electronic environment at the iron, the carbonyl bond distance measurements only indirectly reflect these changes. Similar

(20) Davison, A.; Traficante, D. D.; Wreford, S. S. *J. Am. Chem. Soc*. **1974**, *96*, 2802.

(21) Jacobsen, G. B.; Andersen, E. L.; Housecraft, C. E.; Hong, F. E.; Buhl, M. L.; Long, G. J.; Fehlner, T. P. *Inorg. Chem*. **1987**, *26*, 4040.

(22) Vites, J.; Housecraft, C. E.; Eigenbrat, C.; Buhl, M. L.; Long, G. J.; Fehlner, T. P. *J. Am. Chem. Soc*. **1986**, *108*, 3304.

(23) Housecraft, C. E.; Buhl, M. L.; Long, G. J.; Fehlner, T. P. *J. Am. Chem. Soc*. **1987**, *109*, 3323.

(24) Davis, B. R.; Bernal, I.; Buttone, J.; Good, M. L. *Moessbauer Eff. Methodol*. **1973**, *8*, 127.

(25) Birchall, T.; Drummond, I. *Inorg. Chem*. **1971**, *10*, 399.

Table 7. Selected X-ray Bond Distances and Mössbauer Spectral Isomer Shifts for Compounds **1**, **2**, **5**, and **6**

compound	CO distance (Å)	Fe−C(O) distance (Å)	isomer shift δ(78 K)	ref
[Fe(η^5-C_5H_5)(CO)$_2$$B_5H_7$P($C_6H_5$)$_2$] (**1**)	1.157(4)	1.725(4)	0.024	5
	1.157(4)	1.738(4)		
[Fe(η^5-C_5H_5)(CO)$_2$$B_5H_8$] (**2**)	1.151(4)	1.734(3)	0.039	this work
	1.148(4)	1.738(4)		
[Fe(η^5-C_5H_5)(CO)B_3H_7(P(C_6H_5)$_2$)] (**5**)	1.144(5)	1.758(4)	0.244	6
[Fe(η^5-C_5H_5)(CO)B_5H_8] (**6**)	1.146(5)	1.728(4)	0.04	7b

relationships between the Mössbauer spectral parameters and the ^{11}B NMR data for these complexes, given in Table 6, were also observed.

Conclusions

The Mössbauer effect data for compounds **1**−**6** provide additional information on the electronic distribution and bonding considerations of the borane ligands in organometallic complexes. The conclusions derived from the Mössbauer results are directly supported by the infrared, ^{11}B NMR, and X-ray crystal structural results for these complexes. Compounds **1**−**3** were found to be superior donors compared to their halide, pseudohalide, or alkyl analogues. The Mössbauer spectral results also showed that the [μ-2,3-(P(C_6H_5)$_2$$B_5H_7$]$^-$ ligand is a superior electron donor to the unsubstituted [B_5H_8]$^-$ ligand. The data for compounds **1**, **4**, and **5**, suggest that the borane cage becomes a poorer donor ligand as it becomes progressively smaller. The X-ray crystallographic data for compounds **1**, **2**, **5**, and **6** were also found to agree with the trends observed in the Mössbauer spectral data, which showed that the s-electron density on the iron nucleus increases in the order **5** < **6** < **2** < **1**. The results of this study are also in general agreement with the Mössbauer study of other compounds of the general formula [Fe(η^5-C_5H_5)(CO)LX], where L = CO or PPh_3 and X = halide, pseudohalide, alkyl, or silyl.[2−4]

Acknowledgment. We thank the National Science Foundation (Grant Nos. MSS-89-09793 and CHE-9521572), the National Science Foundation Research Experiences for Undergraduates Site Award (Grant No. CHE-8900471), the Donors of the Petroleum Research Fund, administered by the American Chemical Society, the Wright-Patterson Laboratory (Award No. F33615-90-C-5291), and the Industrial Affiliates Program of the Center for Molecular Electronics for support of this work.

Supporting Information Available: Tables of complete crystallographic data, all atomic coordinates, anisotropic thermal parameters, bond distances and angles involving both non-hydrogen and hydrogen atoms, and intermolecular distances for **2** (12 pages). Ordering information is given on any current masthead page.

IC9605478